Lamb Wave Actuation and Propagation Using Flexoelectric Transducers

SURAJ KUMAR ROUT and SANTOSH KAPURIA

ABSTRACT

In recent years, actuation and propagation using a relatively novel electromechanical effect, namely flexoelectricity, have become an emerging field of research. In this article, we explore the use of flexoelectric dielectrics for Lamb wave actuation and propagation for structural health monitoring (SHM) applications. Towards this objective, an analytical solution is presented for Lamb wave generation and propagation in plate-like structures using flexoelectric-piezoelectric transducers bonded to the host plate surface through an adhesive layer. The model considers both interfacial shear and peel stresses at the interface of the transducer and the plate. These interfacial stresses under applied electric actuation are determined based on a one-dimensional (1D) model, which assumes Kirchhoff plate-like behaviour for both the actuator and the host plate. A 2D elasticity solution is obtained for Lamb wave propagation in the host plate under the interfacial shear and peel stresses obtained from the above 1D model considering plane strain conditions. This solution is obtained in the wave number domain by applying Fourier transform spatially. Finally, the response is obtained in the physical domain by applying the inverse Fourier transform and residue theorem. The strain response at the plate surface is compared with the rigid bonding model to illustrate the effect of bonding compliance. The numerical study demonstrates the effect of the adhesive layer on the response for different excitation frequencies.

INTRODUCTION

Lamb wave-based structural health monitoring (SHM) has been widely adopted for damage detection in thin-walled structures in the last two decades [1]. Among various smart materials, piezoelectric materials have been extensively used as sensors, actuators, and energy harvesters due to their advantages, such as low cost, large bandwidth, high sensitivity, and resistance to electromagnetic fields and radiation. However, this effect is only shown by non-centrosymmetric materials. Also, most piezoelectric materials possess health concerns.

A relatively novel electromechanical coupling effect called flexoelectricity occurring in all dielectric materials is emerging as an alternative to overcome the limitations of piezoelectric materials. This is a higher-order linear electromechanical effect which relates the dipole polarisation to the mechanical strain gradient (direct effect) and mechanical strain to the electric field gradient (converse effect) [2]. Due to the fact that the effect is caused by strain and polarisation gradients, it depends on size. This makes it better than the piezoelectric effect for nano- and micro-scales [3].

Suraj Kumar Rout, PhD Student, Email: suraj.kumar.rout6696@gmail.com. Department of Applied Me- chanics, Indian Institute of Technology Delhi, New Delhi 110016, India
Santosh Kapuria, Professor, Email: kapuria@am.iitd.ac.in; Tel. +91-11-26591218. Department of Ap- plied Mechanics, Indian Institute of Technology Delhi, New Delhi 110016, India

The discovery of large flexoelectric effects has led to a very high surge in the study of flexoelectric structures and devices in the last decade [4]. The use of the converse flexoelectric effect to actuate a host structure has been much less studied. Tzou and coworkers [5] presented a theoretical framework for actuating elastic beams using flexoelectric patch actuators considering rigid bonding model (pin-force-moment). The same group also studied the actuation of rectangular plates using flexoelectric strip actuators. Wang et al. [6] presented a consistent pin-force-moment model for the actuation of host beam using rigidly bonded flexoelectric actuator. Wei et al. [7] extended this model to obtain an analytical solution for Lamb wave generation in plates using flexoelectric actuators. Ray [8] analysed a nanobeam integrated with a rigidly bonded flexoelectric actuator layer using the first order shear deformation theory. In a recent article, the authors [9] have developed a one-dimensional analytical model for actuation using piezoelectric-flexoelectric transducer by considering both interfacial shear and peel stresses.

All the analytical models available so far for Lamb wave actuation and propagation using flexoelectric transducers, considered rigid bonding between the actuator and the host structure. It is well known from earlier studies on piezoelectric actuators that the interfacial stress profiles at the actuator-host structure interface are far from being concentrated at the actuator edges [10], and in turn, have significant effects on the actuation and propagation [11]. Piezoelectric transducers are widely used for actuating and sensing Lamb waves in thin-walled structures for online SHM. While in these transducers, the stress transfer between the transducer and the host plate occurs predominantly through the interfacial shear stress, in flexoelectric transducers, the normal interfacial stress (peel stress) dominates. In this article, we obtained a 2D elasticity solution for Lamb wave propagation in the host plate under interfacial stresses obtained from the above 1D model considering plane strain conditions. The solution is obtained in the wave number domain by applying Fourier transform spatially. Further, the response is obtained in the physical domain by using inverse Fourier transform and residue theorem. This formulation is validated by comparing the forward response with the pin-force-moment model. Finally, the effect of the adhesive layer on forward response has been illustrated for different excitation frequencies.

FLEXOELECTRIC ACTUATOR MODEL

In our previous work [9], we have presented the analytical solution for the interfacial shear and peel stresses at the interface between a flexoelectric-piezoelectric actuator and the host plate. It is briefly recalled in this section. The 3D constitutive relations for a flexoelectric-piezoelectric solid domain are obtained from the bulk electric Gibbs energy density function as

$$\begin{aligned} \boldsymbol{\sigma}^p &= \boldsymbol{C}\boldsymbol{\varepsilon} - \boldsymbol{e}^{\mathrm{T}}\boldsymbol{E} + \boldsymbol{\mu}\boldsymbol{V} \\ \boldsymbol{D}^p &= \boldsymbol{e}\boldsymbol{\varepsilon} + \boldsymbol{\eta}\boldsymbol{E} + \boldsymbol{\mu}\boldsymbol{W} \end{aligned} \tag{1}$$

where $\boldsymbol{\sigma}^p$ and $\boldsymbol{D}^p$ are physical stress tensor and physical electric displacement vector, respectively. $\boldsymbol{\varepsilon}$ and $\boldsymbol{E}$ denote the strain and electric field vector, respectively. $\boldsymbol{C}$, $\boldsymbol{e}$, and $\boldsymbol{\eta}$ are the familiar elastic stiffness coefficients, piezoelectric stress constants, and dielectric permittivity under constant strain, respectively. $\boldsymbol{\mu}$ represent both converse and direct

TABLE I. ESSENTIAL AND NATURAL BOUNDARY CONDITIONS.

Essential	Natural
$u_i = \bar{u}_i$	$(\sigma_{ij} - \tau_{ijk,k})n_j + (\triangle_l n_l)n_j n_k \tau_{ijk} - \triangle_j(\tau_{ijk}n_k) = \bar{t}_i$
$\phi = \bar{\phi}$	$(D_i - Q_{ij,j})n_i + (\triangle_l n_l)n_j n_i Q_{ij} - \triangle_j(Q_{ij}n_j) = \bar{D}_n$
$u_{i,l}n_l = \bar{v}_i$	$\tau_{ijk}n_k n_j = \bar{r}_i$
$\phi_{,k}n_k = \bar{\chi}$	$Q_{ij}n_j n_i = \bar{Q}$

flexoelectric coefficients. $\boldsymbol{V}$ and $\boldsymbol{W}$ are defined as electric field gradient and strain gradient respectively.

The governing equations of motion and the boundary conditions for linear dielectric solids are derived using the extended Hamilton's principle as

$$\begin{aligned} \sigma^p_{ij,j} + b_i &= \rho\ddot{u}_i, \\ D^p_{i,i} &= 0. \end{aligned} \tag{2}$$

where $\sigma^p_{ij} = \sigma_{ij} - \tau_{ijl,l}$ is physical stress tensor and $D^p_i = D_i - Q_{il,l}$ is physical electric displacement vector. σ_{ij} denotes the Cauchy stress tensor, D_k electric displacement vector, τ_{ijl} higher-order stress tensor, and Q_{kl} higher-order electric displacement [12].

The essential and natural boundary conditions are listed in Table I.

where u_i and ϕ_i are displacement vector and electric potential, respectively. b_i, $\bar{t}_i$, $\bar{D}_n$, $\bar{r}_i$, $\bar{Q}$ are the body force components, surface tractions, electric charge density, higher order tractions, and higher order charge, respectively. $\Delta_j = \partial_j - n_j n_l \partial_l$ is the tangential gradient operator.

By using these constitutive relations and governing equations, we developed an analytical model for the interfacial shear and peel stresses between the surface-bonded flexoelectric transducer and host structure (Fig. 1) by satisfying all the boundary conditions. The close-form solutions of the interfacial stresses can be expressed as [9]

$$\tau(x) = C_1 \sinh(px) + C_3 \sinh(\alpha x)\cos(\gamma x) + C_5 \cosh(\alpha x)\sin(\gamma x). \tag{3}$$

$$\begin{aligned} \sigma_z = {} & C_1\delta_1 \cosh(px) + C_3\left[\delta_2 \cosh(\alpha x)\cos(\gamma x) + \delta_3 \sinh(\alpha x)\sin(\gamma x)\right] \\ & + C_5\left[\delta_2 \sinh(\alpha x)\sin(\gamma x) - \delta_3 \cosh(\alpha x)\cos(\gamma x)\right], \end{aligned} \tag{4}$$

where C_1, C_3, and C_5 are the arbitrary constants to be determined from the boundary conditions. δ_1, δ_2, and δ_3 can be defined as

$$\delta_1 = \frac{p(\Gamma_{11} - p^2)}{\Gamma_{12}}, \quad \delta_2 = \frac{\alpha(\Gamma_{11} + 3\gamma^2 - \alpha^2)}{\Gamma_{12}}, \quad \delta_3 = -\frac{\gamma(\Gamma_{11} - 3\alpha^2 + \gamma^2)}{\Gamma_{12}}. \tag{5}$$

ELASTICITY SOLUTION FOR LAMB WAVE PROPAGATION

We consider a model in which a flexoelectric transducer of length 'a' is bonded to a thin isotropic plate through an adhesive layer (Fig. 1). The thickness of the transducer, host plate, and adhesive layer is h_t, h, and, h_a, respectively. The plate has Youngs modulus Y_s and Poissons ratio ν_s, and G_a is the shear rigidity of the adhesive layer.

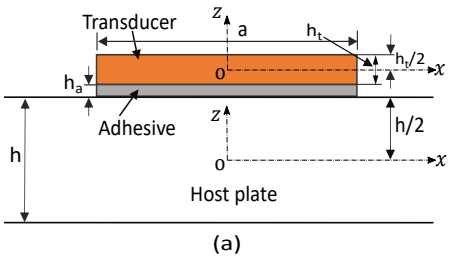

Figure 1. Transducer-adhesive-plate system.

The Lamb wave equations and boundary conditions for an isotropic plate in the wave number domain can be represented under plane strain condition by using Fourier transform as [13]:

$$\tilde{\phi}_{,zz} + m^2\tilde{\phi} = 0, \qquad \tilde{\psi}_{,zz} + n^2\tilde{\psi} = 0 \tag{6}$$

$$\tilde{\sigma}_{zz}|_{z=h/2} = \tilde{\sigma}_z, \quad \tilde{\sigma}_{zz}|_{z=-h/2} = 0, \quad \tilde{\tau}_{zx}|_{z=+h/2} = \tilde{\tau}, \quad \tilde{\tau}_{zx}|_{z=-h/2} = 0 \tag{7}$$

where $m^2 = \dfrac{\omega^2}{{c_L}^2} - k^2$, and $n^2 = \dfrac{\omega^2}{{c_T}^2} - k^2$. c_L and c_T are longitudinal (pressure) and transverse (shear) wave speeds of the bulk material, respectively. k denotes the wave number.

The spatial amplitudes $\tilde{\tau}$ and $\tilde{\sigma_z}$ of τ and σ_z can be obtained by applying Fourier transform to Eqs. (3) and (4), respectively, which are defined as

$$\begin{aligned} \tilde{\tau} &= C_1\tilde{\tau}_1 + C_3\tilde{\tau}_2 + C_5\tilde{\tau}_3 \\ \tilde{\sigma}_z &= C_1\delta_1\tilde{\sigma}_1 + C_3(\delta_2\tilde{\sigma}_2 + \delta_3\tilde{\sigma}_3) + C_5(\delta_2\tilde{\sigma}_3 - \delta_3\tilde{\sigma}_2) \end{aligned} \tag{8}$$

where $\tilde{\tau}_1$, $\tilde{\tau}_2$, and $\tilde{\tau}_3$ are Fourier transforms of $\sinh(px)$, $\sinh(\alpha x)\cos(\gamma x)$, and $\cosh(\alpha x)\sin(\gamma x)$, respectively. Similarly, $\tilde{\sigma}_1$, $\tilde{\sigma}_2$, and $\tilde{\sigma}_3$ resulted from the Fourier transform of $\cosh(px)$, $\cosh(\alpha x)\cos(\gamma x)$, and $\sinh(\alpha x)\sin(\gamma x)$, respectively. The general solution of Eq. (6) can be obtained as

$$\tilde{\phi} = A_1\cos(mz) + A_2\sin(mz), \quad \tilde{\psi} = B_1\cos(nz) + B_2\sin(nz). \tag{9}$$

A_1, A_2, B_1, and B_2 are unknowns to be determined by applying boundary conditions from Eq. (7). The longitudinal displacement and strain in wave number domain can be defined in terms of potential functions as

$$\tilde{u_x} = ik\tilde{\phi} + \tilde{\psi}_{,z}, \quad \tilde{\varepsilon}_x = -k^2\tilde{\phi} + ik\tilde{\psi}_{,z}. \tag{10}$$

Applying inverse Fourier transform to the resulting solution in wave number domain and using the residue theorem, the in-plane strain ε_x at the top surface of the plate is obtained in the physical domain as

$$\varepsilon_x = \varepsilon_x(x, h/2) = \varepsilon_x^S(x) + \varepsilon_x^A(x). \tag{11}$$

TABLE II. MATERIAL PROPERTIES.

Material	Y	G	ν	d_{31}	d_{32}	μ_{19}	μ_{39}	ρ
	(GPa)			($\times 10^{-12}$mV^{-1})		(μC/m)		
Al [14]	70	-	0.33	-	-	-	-	2700
Adhesive [13]	4.7	1.67	-	-	-	-	-	-
BST [7]	150	-	0.3	-47.616	-47.616	8.5	100	-

with

$$\begin{aligned}\varepsilon_x^s(x) &= \frac{1}{2\mu}\sum_{k^S}\frac{\tilde{\tau}(k^S)N_S^{\tau}(k^S)}{D_S^{'}(k^S)}e^{ik^S x} - \frac{i}{2\mu}\sum_{k^S}\frac{\tilde{\sigma_z}(k^S)N_S^{\sigma_z}(k^S)}{D_S^{'}(k^S)}e^{ik^S x}\\ \varepsilon_x^A(x) &= \frac{1}{2\mu}\sum_{k^A}\frac{\tilde{\tau}(k^A)N_A^{\tau}(k^A)}{D_A^{'}(k^A)}e^{ik^A x} - \frac{i}{2\mu}\sum_{k^A}\frac{\tilde{\sigma_z}(k^A)N_A^{\sigma_z}(k^S)}{D_S^{'}(k^S)}e^{ik^A x}\end{aligned} \tag{12}$$

where μ is Lame constant and

$$\begin{aligned}N_S^{\tau}(k) &= kn(k^2+n^2)\cos(mh/2)\cos(nh/2)\\ D_S(k) &= (k^2-n^2)^2\cos(mh/2)\sin(nh/2) + 4k^2mn\sin(mh/2)\cos(nh/2)\\ N_S^{\sigma_z}(k) &= k^2(k^2-n^2)\cos(mh/2)\sin(nh/2) + 2k^2mn\sin(mh/2)\cos(nh/2)\\ N_A^{\tau}(k) &= -kn(k^2+n^2)\sin(mh/2)\sin(nh/2)\\ D_A(k) &= (k^2-n^2)^2\sin(mh/2)\cos(nh/2) + 4k^2mn\cos(mh/2)\sin(nh/2)\\ N_A^{\sigma_z}(k) &= k^2(k^2-n^2)\sin(mh/2)\cos(nh/2) + 2k^2mn\cos(mh/2)\sin(nh/2)\end{aligned} \tag{13}$$

Similarly we can obtain the expression for the displacement u_x in the physical domain.

RESULTS AND DISCUSSION

VALIDATION

To validate the present analytical model, the obtained results are compared with the pin-force-moment (rigid bonding) model by considering both interfacial shear and peel stresses. For this purpose, barium strontium titanate (BST) is chosen as the surface-bonded transducer having a length of 14 mm. Unless stated otherwise, the thickness of the transducer and host plate is taken as 0.1 mm and 1.6 mm, respectively. The material properties for host plate, transducer, and adhesive are listed in Table II. All the results are obtained by considering plane strain condition for both the transducer and the host plate.

The BST patch transducer is actuated with a Hann window modulated five cycle tone burst signal of 20 V amplitude. The input signal is given by $V(t) = \frac{V_o}{2}[1 - \cos(2\pi t/T_H)]\sin(2\pi f t)$, where f denotes the central frequency of the excitation and T_H represents the Hann window length related to the number of cycles N_B in the tone burst as $T_H = N_B/f$.

First, to validate the proposed model in respect of Lamb wave generation and propagation, the in-plane stain ε_x generated at the top surface of the plate at a distance of 300 mm from the center of the actuator, is compared in Fig. 2 with the rigid bonding model.

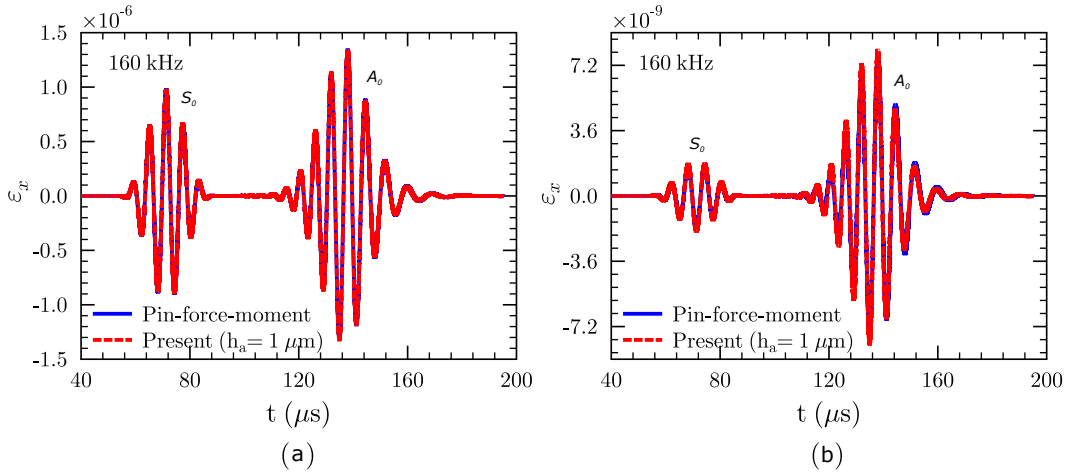

Figure 2. Longitudinal strain ε_x at the top surface of the host plate at a distance of 300 mm for actuation under five-cycle modulated tone burst excitation of 160 kHz central frequency considering (a) piezoelectric effect and (b) flexoelectric effect

For this, we have considered an adhesive of 1 μm thickness. For excitation input signal of 160 kHz central frequency is considered. The results illustrated in Figs. 2 (a) and (b) are obtained by considering the piezoelectric effect and flexoelectric effect, respectively. For both the cases, the amplitudes of both S_0 and A_0 modes show an excellent agreement with the pin-force-moment model solution.

EFFECT OF ADHESIVE THICKNESS ON THE RESPONSE

In this section, we study the effect of adhesive thickness (h_a) on the Lamb wave response ε_x for two different central frequencies. The results are obtained at a distance stated previously by considering only the flexoelectric effect.

Figure 3 illustrates the effect of adhesive thickness on ε_x for 100 and 300 kHz excitations. For 100 kHz, we can see from the graph, there is no difference in the waveform of S_0 mode as the adhesive thickness increases. However, for 300 kHz, the waveform of S_0 mode slightly changes for adhesive thickness 60 μm (Fig. 3 (b)). On the other hand, for both frequencies, the amplitude of A_0 mode decreases as we increase the adhesive thickness up to 20 μm. Subsequently, a further increase in the adhesive thickness does not affect the amplitude of A_0 mode.

CONCLUDING REMARKS

In this article, we have developed an analytical model for Lamb wave propagation in plate-like structures using flexoelectric-piezoelectric transducers bonded to the top surface of the host structure through an adhesive layer. In this model, we have considered both interfacial shear and peel stresses at the interface of the transducer and plate. A two dimensional elasticity solution is obtained for Lamb wave propagation in the host plate under the interfacial stresses obtained from our previous work considering plane strain

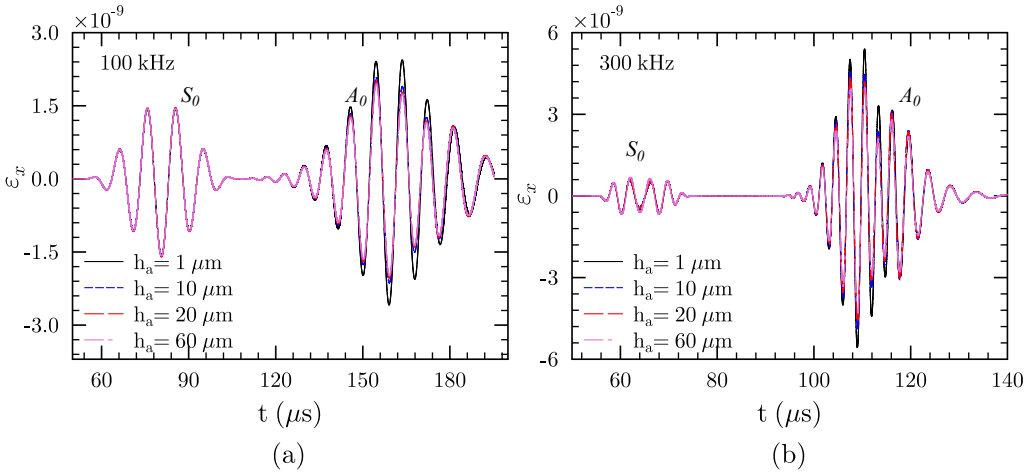

Figure 3. Effect of adhesive thickness h_a on longitudinal strain ε_x at the top surface of the host plate at a distance of 300 mm under five-cycle Hann window modulated tone burst with central frequency of (a) 100 kHz and (b) 300 kHz considering flexoelectric effect

conditions.

The Lamb wave response obtained with a very thin adhesive layer of 1 μm thickness is found to match with the pin-force-moment model by considering piezoelectric and flexoelectric effects separately. For 100 and 300 kHz excitations, the S_0 mode waveform does not show any significant variation with the increase in adhesive thickness. However, the amplitude of A_0 mode is significantly altered by the adhesive thickness upto 20 μm for this study beyond which it does not show much change with the increase of adhesive thickness.

REFERENCES

1. Giurgiutiu, V., B. Lin, G. Santoni-Bottai, and A. Cuc. 2011. "Space application of piezoelectric wafer active sensors for structural health monitoring," *Journal of Intelligent Material Systems and Structures*, 22(12):1359–1370.
2. Tagantsev, A. 1985. "Theory of flexoelectric effect in crystals," *Zhurnal Eksperimental'noi i Teoreticheskoi Fiziki*, 88(6):2108–22.
3. Majdoub, M., P. Sharma, and T. Cagin. 2008. "Enhanced size-dependent piezoelectricity and elasticity in nanostructures due to the flexoelectric effect," *Physical Review B*, 77(12):125424.
4. Jiang, X., W. Huang, and S. Zhang. 2013. "Flexoelectric nano-generator: Materials, structures and devices," *Nano Energy*, 2(6):1079–1092.
5. Deng, B., H. Li, and H. Tzou. 2015. "Optimal positions for multiple flexoelectric actuations on beams," in *ASME International Mechanical Engineering Congress and Exposition*, American Society of Mechanical Engineers, vol. 57564, p. V013T16A008.
6. Wang, Z., Z. Xie, and W. Huang. 2018. "A pin-moment model of flexoelectric actuators," *International Journal of Hydromechatronics*, 1(1):72–90.
7. Wei, C., Z. Wang, and W. Huang. 2021. "Performance of a flexoelectric actuator for Lamb wave excitation," *Journal of Applied Physics*, 129(3):034902.

8. Ray, M. 2017. “Mesh free model of nanobeam integrated with a flexoelectric actuator layer,” *Composite Structures*, 159:63–71.
9. Rout, S. K. and S. Kapuria. 2023. “A flexoelectric actuator model with shear-lag and peel stress effects,” *Proceedings of the Royal Society A*, 479(2273):20230099.
10. Kapuria, S. and P. Kumari. 2013. “Extended Kantorovich method for coupled piezoelasticity solution of piezolaminated plates showing edge effects,” *Proceedings of the Royal Society A: Mathematical, Physical and Engineering Sciences*, 469(2151):20120565.
11. Agrahari, J. and S. Kapuria. 2016. “Effects of adhesive, host plate, transducer and excitation parameters on time reversibility of ultrasonic Lamb waves,” *Ultrasonics*, 70:147–157.
12. Polizzotto, C. 2016. “A note on the higher order strain and stress tensors within deformation gradient elasticity theories: Physical interpretations and comparisons,” *International Journal of Solids and Structures*, 90:116–121.
13. Kapuria, S., B. N. Sharma, and A. Arockiarajan. 2022. “Role of transducer inertia in generation, sensing, and time-reversal process of Lamb waves in thin plates with surface-bonded piezoelectric transducers,” *Journal of Intelligent Material Systems and Structures*, 33(6):779–798.
14. Ha, S. and F.-K. Chang. 2009. “Optimizing a spectral element for modeling PZT-induced Lamb wave propagation in thin plates,” *Smart Materials and Structures*, 19(1):015015.